

## EVALUATION OF THERMAL FLUIDS IN THE NORTHWESTERN CHIMBORAZO PROVINCE, ECUADOR

**Amanda Elisa Viteri Nolivos**

Geological and Energy Research Institute IIGE  
De las Malvas E15-142 and de los Perales - Monteserrín  
170503, Quito  
ECUADOR  
*amanda.viteri@geoenergia.gob.ec*

### ABSTRACT

This study uses geochemical methods to evaluate the geothermal potential in the northwestern Chimborazo province through the characterization of thermal waters collected from 1984 to 2016. With this unique dataset, the minimum temperatures of the resources were estimated, and the geothermal fluid production properties evaluated. The results confirm the existence of a low enthalpy geothermal reservoir, whose use has to date been limited to balneology. The alkaline Cl-Na mature waters suggest reservoir temperatures of 70-102°C. The waters at the edge of the geothermal reservoir are alkaline HCO<sub>3</sub> with estimated temperatures of 77-99°C. Both sources have direct use potential in applications such as greenhouse air conditioning.

### 1. INTRODUCTION

Geothermal exploration in Ecuador began in 1978 by the Ecuadorian Institute of Electrification (INECEL). Since then, exploratory studies have been conducted intermittently, however, they have resulted in a better understanding of the country's existing geothermal resources. The most significant advances in geothermal exploration have been made during the last thirteen years, following the reform to the Magna Carta in 2008 (National Assembly of Ecuador, 2008). Since then, the Ecuadorian government has promoted the exploitation and development of high and low enthalpy geothermal energy resources through the allocation of public funds (Asimbaya, 2018). The support of the Japan International Cooperation Agency (JICA) has enabled new exploration projects such as the successful drilling of the first deep exploratory well in Chachimbiro, Imbabura province, in 2017 (Figure 1).

According to the preliminary geothermal exploration studies, there are prospects with moderate to high potential in the Ecuadorian Andes region; however, these areas are for the most part in the early stage of recognition (IAEA, 1992; Beate, 2010; Beate et al., 2020). In addition to Chachimbiro, there are three other high-temperature prospects that are almost ready for deep exploratory drilling, Chacana-Jamanco, Chacana-Cachiyacu, and Tufiño-Chiles, as well as the low temperature prospect of Chalpatán. Six other prospects require completion of pre-feasibility studies to determine where deep exploratory wells need to be drilled. These prospects include Chalupas, Guapán, Chimborazo, Chacana-Oyacachi, Baños de Cuenca, and Alcedo (Figure 1).

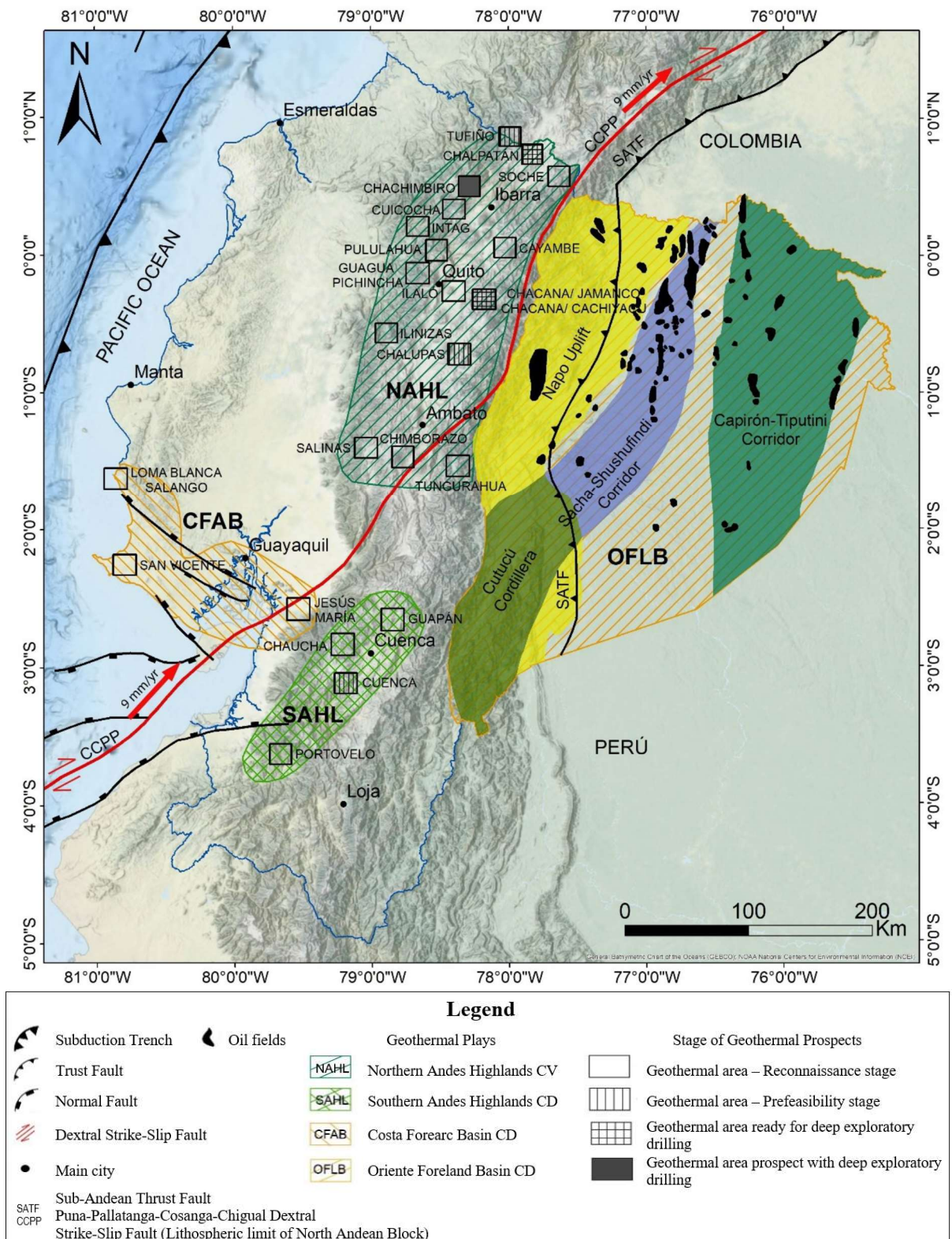


FIGURE 1: Location map of geothermal prospects in Ecuador (Beate et al., 2020)

In the context of the governmental efforts to utilize geothermal resources (MEER, 2010), Chimborazo has been considered one of the national priority prospects for electricity generation. The current energy mix in Ecuador consists of hydropower (58.44%), fossil fuels (23.41%), thermal turbo gas (10.57%), and others (7.58%), with a total installed capacity of 8725 MWe. Only 25,428 GWh from the gross energy production of 32,295 GWh is generated from renewable energy sources (as of August 2021; ARCERNNR, 2021)

The first greenhouse in the Chimborazo province was built in 2018 under the auspices of the Spanish Agency for International Development Cooperation (AECID) and utilizes low-temperature geothermal water. The objective of this project was to determine the optimal conditions for the cultivation of agricultural products, and to evaluate their production performance, energy consumption, and economic, social, and environmental impacts (IIGE, 2020; Urresta et al., 2021). Currently, the utilization of geothermal energy is still limited to direct use in swimming pools (5.16 MWt and 102.4 TJ/yr for annual utilization; Beate et al., 2020).

To estimate and evaluate the capacity of a geothermal system, different methods are applied simultaneously, such as geological, hydrogeological, geochemical, and geophysical methods (Muffler et al., 1978; Barbier, 2002; Gehringer and Loksha, 2012; Romano and Liotta, 2020). So far, no geophysical survey has been completed, and only a few geochemical and hydrogeological surveys have been carried out in the Chimborazo geothermal prospect and its surroundings. The results show the existence of a geothermal reservoir, evidenced by thermal springs, underground water resources, and rock permeability (IAEA, 1992; Carrasco and Naula, 2012; Burbano et al., 2013; Reino, 2013; Ibarra et al., 2015; Jimbo, 2016).

The aim of this research is to use geochemical methods to further evaluate the geothermal potential in the northwestern Chimborazo province through the characterization of the thermal waters collected from 1984 to 2016. With the dataset collected from the study area, the minimum temperatures of the resources were estimated, and the geothermal fluid production properties evaluated.

## **2. STUDY AREA**

### **2.1 Overview of Ecuador's geographical and geological setting**

Ecuador is a democratic republic, located in the western hemisphere in the northwest of South America. Its capital is Quito and the area of the country is 257 217.07 km<sup>2</sup> (Lazo, 2015). This country has diverse climates and ecosystems as a result of the Andes Mountains crossing the country from north to south, thus dividing continental Ecuador into three regions: Coast, Sierra, and Oriente (Beate, 2010; Lazo, 2015).

In the northern part of the Sierra region, the Andes are divided into two parallel mountain ranges (Eastern and Western). These mountain ranges were formed early in the Cenozoic era, in a process of subduction of the Nazca plate under the South American plate. Both mountain ranges have been raised, folded, and are covered by Tertiary and Quaternary volcanic material. This area is also characterized by an active, extensive, and well-developed continental volcanic arc with a calc-alkaline affinity, related to the Nazca subduction. According to the Geophysical Institute of the Polytechnic School of Ecuador, to date there are 27 potentially active volcanoes in Ecuador, including the volcanoes of the Galapagos Islands. Of these, seven continental volcanoes and seven Galápagos volcanoes have had eruptions in historical times, that is, since 1532 (Inguaggiato et al., 2010; EPN, 2021).

Unlike the north, the southern Sierra does not have well-defined mountain ranges (Beate, 2010; Inguaggiato et al., 2010). The Inter-Andean Valley is in the middle of this area and includes many volcanic and epiclastic sedimentary sequences of recent to late Tertiary age. Currently, the edges of the Inter-Andean Valley are defined by superimposed and sub-parallel active inverse faults (Beate, 2010; Inguaggiato et al., 2010).

The Oriente is an extensive sedimentary basin which covers the Precambrian cratonic basement (Baldock, 1982). The oldest rocks include batholiths and associated volcanic products of the Jurassic age, and a Cretaceous carbonate platform covered by Tertiary epiclastic sediments. Large sloping faults of north-south orientation delimit the basin to the west (Tschopp, 1953). Along the western margin of the basin, in a back-arc environment, there is a row of quaternary volcanoes of alkaline affinity, some potentially active (Beate, 2010; Inguaggiato et al., 2010).

The Coast is a flat region located between the Andes and the Pacific Ocean without active volcanism (Beate, 2010; Inguaggiato et al., 2010). It comprises of an ante-arc sedimentary basin of late Cretaceous to Cenozoic age, underlain by oceanic crust from the middle to late Mesozoic (Benítez, 1995; Vallejo et al., 2009).

## 2.2 Generalities of study area

The study area (Figure 2) is located between two provinces in the center of the Sierra, most of which is in the northwest of the Chimborazo province and the rest in the parish of Pilahuín, Tungurahua province. In this area are the volcanoes Chimborazo, Carihuairazo, Tungurahua, and El Altar. This area contains the original geothermal prospect of Chimborazo with an area of 42 km<sup>2</sup>, as defined by Beate (2010), which was extended in this study to the southeast (by approximately 427 km<sup>2</sup>) around the city of Riobamba to the town of Guayllabamba, southeast of the city of Chambo.

The topography is varied with steep and mountainous slopes and the Inter-Andean valley characterized by low hills and wide valleys where most of the samples for this study were taken. The elevation ranges from 135 to 6310 m a.s.l. and the highest elevation corresponds to the top of the Chimborazo volcano. There is rainfall all year round, but the climate is generally drier from July to September (GAD Chimborazo, 2015; GAD Tungurahua, 2015). The whole area is connected by a good road infrastructure to Riobamba, the capital of Chimborazo.

The main cities are Ambato, Riobamba, Villa La Unión, and Chambo, with populations of 329,856, 146,324, 2,313, and 11,885, respectively (INEC, 2021). The main activities that dominate the economic sector in the study area are agriculture, animal husbandry, silviculture, and fish farming (GAD Chimborazo, 2015; GAD Tungurahua, 2015).

Within the study area are two hot springs intended for balneology. One is located on the northern flank of the Chimborazo volcano (Kunugyaku hot springs) and the other towards the extreme southeast of the study area, in Guayllabamba (San Francisco-Guayllabamba hot springs) (GAD Chimborazo, 2015; GAD Tungurahua, 2015).

## 3. METHODOLOGY

The samples that we use here were not collected and analysed during this study. Only limited information regarding sampling and analysis was found in the literature. Therefore, this investigation is based on chemical compositions provided in previous studies.

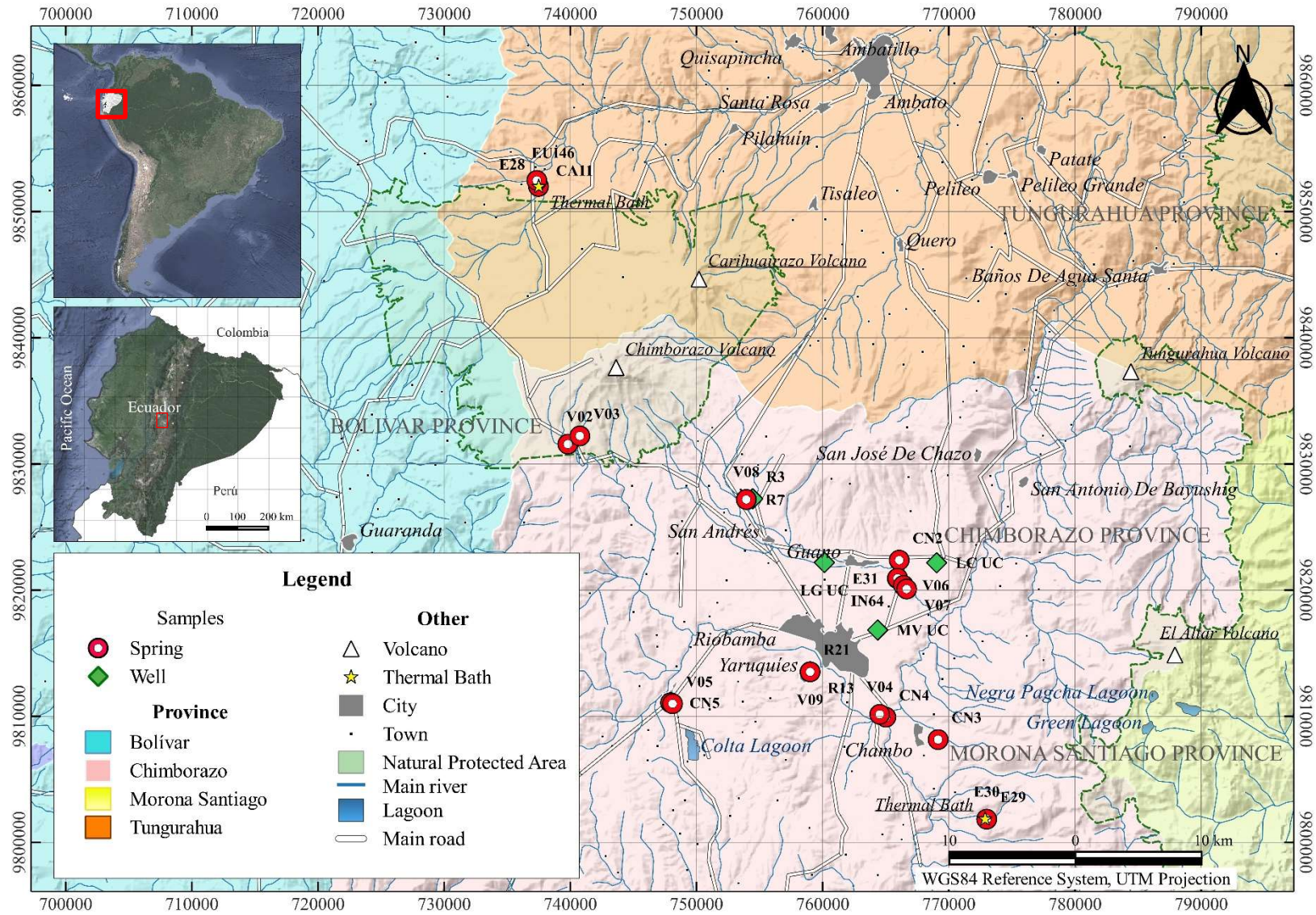


FIGURE 2: Location of study area and fluid sample locations

### 3.1 Fluid classification

A general classification of water types by dominant ions is a quick method to weed out unsuitable samples. Classifying these fluids is a useful tool to investigate the origin and behavior of geothermal fluids and to identify mixing processes or other changes that could alter the composition of primary thermal water (Muffler and Cataldi, 1978; Arnórsson et al., 1983; D'Amore et al., 1983; Giggenbach, 1991; Arnórsson, 2000). They may even provide some indication of the geographic grouping of the fluids (Giggenbach, 1991).

This method consists of grouping the waters according to their cationic and anionic content. The predominance of an ion provides information as to the origin and dynamics of a fluid (D'Amore et al., 1983; Giggenbach, 1988). For example, high Na or Li content suggest the presence of geothermal fluid, in contrast to high Ca and Mg concentrations that indicate the influence of cold waters (IGME, 1985).

For water classification and geothermometry application, the liquid analysis spreadsheet by Powell and Cumming (2010) was used. Using this spreadsheet, the ternary diagrams are generated from measured concentrations of chemical species using formulas based on equilibrium reactions and empirical relationships. The spreadsheet includes tabulated water chemistry data in ppm by weight and tabulates geothermometers. Explanations for the calculations are referenced and a brief description is included in the Powell and Cumming publication.

#### 3.1.1 Piper-Hill-Langelier diagram

The Piper-Hill-Langelier diagram (a.k.a. Piper diagram) shows the percentages of six ion groups in two ternary plots and a diamond plot. A ternary diagram in the lower left represents the cations: K, Ca, and Mg. A ternary diagram in the lower right represents the anions:  $\text{HCO}_3$ ,  $\text{SO}_4$ , and Cl. A central rhomboidal field that unifies the composition deduced from these ions is located between both. In this way, the diagram shows the essential chemical character of a fluid according to the relative composition of its constituents, but not according to absolute concentrations. The waters can thus be grouped into well-defined areas. Further descriptions can be found in Piper (1944).

According to Giggenbach (1991), the main disadvantage of the Piper diagram is the use of sums of constituents, thus erasing any information carried by an individual constituent. The interpretive value of these diagrams is minimal if applied to geothermal waters as it does not provide information on source components, formation processes, or thermodynamic correlations (Giggenbach, 1991). However, in this study the diagram is used to obtain a general overview of the types of fluids in the area.

#### 3.1.2 Ternary diagram Cl-SO<sub>4</sub>-HCO<sub>3</sub>

The ternary diagram Cl-SO<sub>4</sub>-HCO<sub>3</sub> provides information about the probable origin of the fluids and can give indications which samples are more suitable for the application of geothermometry. The position of the data points in this diagram are calculated from the relative concentrations (in mg/kg) of all three constituents involved (Giggenbach, 1991).

In this way, fluids can be classified into four groups: volcanic, steam heated, mature, and peripheral waters. Mature waters are fluids of neutral characteristics dominated by Cl and most likely to represent well-balanced fluids from the main flow zones to the surface. Volcanic and steam-heated waters are formed by the absorption of high-temperature "geothermal" vapors which contain HCl or low-temperature vapors containing H<sub>2</sub>S into groundwater. Volcanic waters generally have sulfated, highly acidic characteristics. Peripheral waters, as the name implies, are found on the peripheries of hydrothermal or cooling systems (Giggenbach, 1991).

The most suitable group for the application of further geochemical calculations and geothermometry are the neutral “geothermal” waters, which are low in  $\text{SO}_4$ , high in Cl, and located along the Cl- $\text{HCO}_3$  axis, near the corner of Cl. In the case of neutral waters with high bicarbonate content, considerable caution is required in the application of most geoindicators (Arnórsson, 2000; Giggenbach, 1991).

### 3.2 Reservoir temperature estimation

Geothermometers are defined as mathematical relationships that calculate the temperature of a geothermal reservoir at depth based on the chemical composition of the fluid (Giggenbach, 1991; Powell and Cumming, 2010). According to Arnórsson (2000), geothermometry is probably the most important tool during the exploration and development of geothermal resources. It is also crucial during the utilization stage since it helps monitor the response of geothermal reservoirs to the production load.

Geothermometers are classified into three groups: solute, gas, and isotopes (Arnórsson, 1985). The most important solute geothermometers are silica (quartz and chalcedony), Na/K, and Na-K-Ca. Others that have been developed are based on the ratios of Na/Li, Li/Mg, K/Mg and Na-K-Mg (Arnórsson, 2000).

#### 3.2.1 Na-K-Mg geothermometer

Giggenbach (1986) proposed a combination of two mineral sub-systems, Na-K and K-Mg geothermometers, in a ternary diagram that classifies thermal water into immature, partially or totally equilibrated waters. The zone of partial equilibrium suggests either that a mineral assemblage composed of albite, K-feldspar, muscovite, and clinocllore has dissolved but has not reached equilibrium, or that a mixture of water that has reached equilibrium (e.g., geothermal water) is diluted with immature water (e.g., cold groundwater) (Giggenbach, 1988). Data points near the corner of  $\sqrt{\text{Mg}}$  (referred to as Mg in this geothermometer) generally show a high proportion of relatively cold groundwater, but are not necessarily “immature” water (Giggenbach, 1991).

The ternary diagram displays the cations Na, K, and Mg expressed in mg/kg in the vertexes of the triangle. Like the Cl- $\text{SO}_4$ - $\text{HCO}_3$  diagram, the position of each data point is determined by the relative concentrations of the three cations.

The diagram can then be used to extrapolate the possible temperature of the reservoir based on the Na-K and K-Mg geothermometers. This allows the evaluation of deeper equilibrium temperatures and the effects of a variety of processes such as rebalancing and mixing of waters of different origins for many samples. Moreover, the diagram helps to make a clear distinction between suitable or inadequate waters for the application of geothermometers of ionic solutes. For more reliable results, it is advisable to first make an initial evaluation of the samples according to their pH or their relative content of Cl- $\text{SO}_4$ - $\text{HCO}_3$ . Further descriptions of this diagram can be found in Giggenbach (1991).

#### 3.2.2 Solute geothermometers

Many water/solute geothermometers and their calibrations were developed from the mid-1960s to the mid-1980s. The most important ones are the silica (quartz and chalcedony) and cation geothermometers (Arnórsson, 2000). The reservoir temperature in this study was estimated using six different geothermometers of silica: amorphous silica,  $\alpha$ -cristobalite,  $\beta$ -cristobalite, chalcedony conductive, and quartz conductive and adiabatic, as well as nine cation geothermometers: Na-K-Ca, Na-K-Ca-Mg corrected, K/Mg, and several Na-K geothermometers. The main empirical equations for the specific geothermometers are detailed in Table 1 and information on the principles and chemical reactions of each can be found in the relevant publication.

TABLE 1: Empirical equations of aqueous geothermometers (Powell and Cumming, 2010)

Geothermometer	Reference	Empirical equation	Applicability (°C)
Amorphous Silica	Fournier, 1977	$T = \frac{731}{4.52 - \log \text{SiO}_2} - 273.15$	0-250
$\alpha$ -Cristobalite	Fournier, 1977	$T = \frac{1000}{4.78 - \log \text{SiO}_2} - 273.15$	0-250
$\beta$ -Cristobalite	Fournier, 1977	$T = \frac{781}{4.51 - \log \text{SiO}_2} - 273.15$	0-250
Chalcedony conductive	Fournier, 1977	$T = \frac{1032}{4.69 - \log \text{SiO}_2} - 273.15$	0-250
Quartz conductive	Fournier and Potter, 1982	$T = \frac{1309}{5.19 - \log \text{SiO}_2} - 273.15$	Up 330
Quartz adiabatic	Fournier, 1981	$T = \frac{1522}{5.75 - \log \text{SiO}_2} - 273.15$	Up 330
*Na-K-Ca	Fournier, 1981	$T = \frac{1647}{\log \frac{\text{Na}}{\text{K}} + \left( \beta \log \frac{\sqrt{\text{Ca}}}{\text{Na}} + 2.06 \right) + 2.47} - 273.15$	
		$T = T_{\text{Na-K-Ca}} - \Delta T_{\text{Mg}}$	
		$R = \frac{\text{Mg}}{\text{Mg} + 0.61\text{Ca} + 0.31\text{K}} \times 1000$	
Na-K-Ca-Mg	Fournier, 1981	$\Delta T_{\text{Mg(R 1.5-5)}} = \frac{-1.03 + 59.971 \log R + 145.05 \log R^2 - 36711 \log R^2}{T - 1.67 \times 10^7 \frac{\log R^3}{T^2}}$	
		$\Delta T_{\text{Mg(R 5-50)}} = \frac{10.66 + 4.7415 \log R + 325.87 \log R^2 - 1.032 \times 10^5 \log R^2}{T - 1.9677 \frac{\log R^3}{T^2}}$	
Na-K	Fournier et al., 1979	$T = \frac{1217}{\log \frac{\text{Na}}{\text{K}} + 1.483} - 273.15$	
Na-K	Truesdell, 1976	$T = \frac{855.6}{\log \frac{\text{Na}}{\text{K}} + 0.8573} - 273.15$	100-275
Na/K	Giggenbach, 1988	$T = \frac{1390}{1.75 - \log \frac{\text{Na}}{\text{K}}} - 273.15$	
Na/K	Tonani, 1980	$T = \frac{833}{0.78 - \log \frac{\text{Na}}{\text{K}}} - 273.15$	
Na/K	Nieva and Nieva, 1987	$T = \frac{1178}{1.47 - \log \frac{\text{Na}}{\text{K}}} - 273.15$	
Na/K	Arnórsson et al., 1983	$T = \frac{933}{0.993 - \log \frac{\text{Na}}{\text{K}}} - 273.15$	25-250
K/Mg	Giggenbach, 1986	$T = \frac{4410}{13.95 - \log \frac{\text{K}^2}{\text{Mg}}} - 273.15$	

\* $\beta=4/3$  for  $T < 100^\circ\text{C}$  and the term  $\log \frac{\sqrt{\text{Ca}}}{\text{Na}} + 2.06$  is positive, then  $\beta=4/3$ , otherwise  $\beta=1/3$



### 3.3 Geochemical calculations

The aqueous speciation and chemical composition calculations simulate the chemical reactions and processes that determine the chemical characteristics of the thermal fluid in depth (Arnórsson, 2000). These calculations are performed in geothermal chemistry programs that permit calculation of individual aqueous species activities. The most common programs that do these and other calculations are EQ3/6, SOLVEQ/CHILLER, Geochemist's Workbench, WATEQ4F, WATCH, and PHREEQC (Cioni and Marini, 2020); the latter two were used in this work.

Using the WATCH software (Arnórsson et al., 1982; Bjarnason, 2010), the reference temperature was calculated based on the chalcedony geothermometer, which is generally applicable in low-temperature hot springs (Fournier, 1977). Therefore, ten samples with complete compositions including SiO<sub>2</sub> were used to estimate the deep aquifer temperature. In the calculations, the minimum concentrations of Al and Fe (0.001 ppm) were assumed for samples lacking this data. The CO<sub>2</sub> concentrations were calculated from pH and HCO<sub>3</sub> concentrations, used the following equations (Drever, 1988):

$$\log K_1 = 1.1 \cdot 10^{-4}T^2 + 0.012T + 6.58 \quad (1)$$

$$\log K_2 = 9 \cdot 10^{-5}T^2 + 0.037T + 10.62 \quad (2)$$

where  $K_1$  = Equilibrium constant 1;  
 $K_2$  = Equilibrium constant 2; and  
 $T$  = Temperature of the sample [°C].

Finally, TDS concentrations were calculated based on the linear correlation of this parameter with EC (Rusydi, 2018):

$$\text{TDS} = k * \text{EC} \quad (3)$$

where TDS = Total dissolved solids [mg/L];  
 EC = Electrical conductivity [ $\mu\text{S}/\text{cm}$ ]; and  
 k = Ratio TDS/EC, for freshwater this ratio is 0.65.

The reference temperatures calculated in WATCH and the surface fluid compositions were then entered into the PHREEQC program (Parkhurst et al., 1980). In PHREEQC, the carfix thermodynamic database (Voigt et al., 2018) was used to calculate pH and the mineral saturation indices, which represents the saturation state of the water with respect to a mineral. Comparison between the reaction quotient (Q) and the equilibrium constant (K) permits evaluation of this state of equilibrium, that is, the mineral saturation index (SI), and is given by the following equation:

$$\text{SI} = \log \frac{Q}{K} \quad (4)$$

If the SI is negative, it follows that the mineral is unsaturated and if present could dissolve. Conversely, if the SI is positive, the mineral is oversaturated and could precipitate as a result (Arnórsson, 2000).

Geothermal waters can be conductively cooled by heat loss as they ascend from the reservoir through cooler rocks up to the surface or by boiling due to decreased hydrostatic charge. Conductive cooling does not by itself cause any change in the chemical composition of the water. However, cooling can change its degree of saturation with respect to primary and secondary minerals. As a result, conductive cooling can modify the chemical composition of rising water by dissolution or mineral precipitation (Arnórsson, 2000). To establish water saturation states with respect to various minerals at different

temperatures, conductive cooling calculations from 80°C to 5°C were also completed for each sample in PHREEQC assuming that the utilization of this water will cool it down. The evaluation of changes in the saturation states is useful for assessing trends in potential scaling of minerals, such as calcite and amorphous silica, in wells and surface equipment (Arnórsson, 2000).

## 4. RESULTS AND DISCUSSION

### 4.1 Chemical composition

Geochemical information from 29 geothermal fluid samples was collected from literature published between 1992 and 2016 (Table 2, Appendix I). The chemical composition of the samples is shown in Table 3. Samples R3, R13, and MV UC were collected from wells that supply drinking water (for public-home use, suitable for food and domestic use), and irrigation, samples R7 and R21 were collected from streams and the rest of the samples from springs (Figure 2).

TABLE 2: Investigations included in the present study

Nº	Reference	Title	Type	Nº of samples
1	OIEA, 1992	Geothermal investigations with isotope and geochemical techniques in Latin America	Report	1
2	Inguaggiato et al., 2010	Geochemical and isotopic characterization of volcanic and geothermal fluids discharged from the Ecuadorian volcanic arc	Journal Article	4
3	Carrasco and Naula, 2012	Characterization and Elaboration of an Inventory of Geothermal Sources of Low Enthalpy in the Province of Chimborazo and Proposal for the Creation of a Geothermal Energy Research Center in the ESPOCH	Thesis	4
4	INAMHI, 2013	Thermomineral waters in Ecuador	Report	1
5	Reino, 2013	Study of the groundwater of the city of Riobamba and its areas of influence: Baseline	Thesis	4
6	*Jimbo, 2016	Preliminary geological-geochemical evaluation of the geothermal prospect "Chimborazo", with application of remote sensors	Thesis	13
7	Carrera et al., 2016	Hydrogeochemical analysis of volcanic and geothermal fluids in the Andes from Ecuador using hydrochemical plots (Stiff, Piper and Schoeller-Berkaloff diagrams)	Journal Article	2

\* The document contains information collected by the Ecuadorian Institute of Hydraulic Resources (INHERI) in 1984.

The sampling temperature ranged from 8.5 to 47.5°C, from which three groups of defined ranges can be observed. The first, with a minimum temperature of 8.5°C and a maximum of 11.6°C, is located on the southern flank of the Chimborazo volcano and northwest of San Andrés. The second group has an average temperature of 21°C and is located near Riobamba. The last group has a minimum temperature of 37.6°C and a maximum of 47.5°C. These samples are located at the western and eastern ends of the study area.

The average pH is 7.15. The samples are mostly neutral with a slight tendency to basicity. The E30 sample (located between Guano and Riobamba) is the one with the highest acidity (pH=5.69) and the

lowest EC (83  $\mu\text{S}/\text{cm}$ ), compared to the other samples. Similar values have been reported for sample R7 (pH=5.78). The pH of the samples R3, CN4, LG UC, CA10, CN2, R21, E29, CN3, and 72M19 range between 6.2 and 6.9. All of them are in the surroundings of Riobamba, Chambo and Guayllabamba (San Francisco hot spring). Of this group of samples with slightly acidic characteristics, only one, LG UC, belongs to a well (whose depth is not specified in Ibarra et al., 2015 and Jimbo, 2016).

TABLE 3: Chemical composition of water samples

N°	Code	Type	T	pH	EC	TDS	Na	K	Ca	Mg	SiO <sub>2</sub>	Cl	SO <sub>4</sub>	HCO <sub>3</sub>	CO <sub>2</sub>
			°C		$\mu\text{S}/\text{cm}$	mg/l	mg/l	mg/l	mg/l	mg/l	mg/l	mg/l	mg/l	mg/l	mg/l
1	*72M18		41.0	7.1	2660	1729.0	6.7	0.4	8.0	19.2			4.1	29.4	24
2	*72M19		40.0	6.5	1359	883.4	186.0	15.0	90.2	30.4				775.0	893
3	*EUI46	S	47.5	7.5			682	7.5	320	0.5	48.2	1340.0	252.0	37.9	29
4	*E28	S	47.0	8.4	4300	2795.0	640.9	7.8	299.4	1.0		1289.6	265.6	61.0	45
5	*E29	S	37.6	6.3	1386	900.9	197.1	14.1	103.2	27.8		37.2	0.5	951.9	1291
6	*E30	S	8.6	5.7	83	54.0	5.5	2.3	6.8	3.8		0.4	1.0	67.1	350
7	*E31	S	20.1	7.5	1804	1172.6	186.0	10.6	85.0	120.6		24.8	720.9	439.3	342
8	CN2	S	21.1	6.6	2150	2040.0	155.7	10.9	105.6	131.6		24.1	171.6	439.2	515
9	CN3	S	37.8	6.2	1477	1052.0	146.2	13.5	164.0	24.4		38.3	27.5	768.6	1211
10	CN4	S	20.3	6.5	776	896.0	87.1	9.2	28.8	18.3		18.4	39.5	305.0	388
11	CN5	S	21.0	7.3	481	556.0	39.8	12.1	89.6	38.4		17.0	40.4	323.3	265
12	IN64	S	22.7	7.8	1938	1253.9	158.8	11.9	84.0	126.9	70.0	28.8	899.5	370.0	279
13	R3	W	11.6	6.4	547	265.0	14.0	2.6	38.4	44.7		12.8	30.0	408.0	606
14	R7	S	10.9	5.8	383	184.6	5.5	9.1	32.0	27.2		14.2	58.0	264.0	1107
15	R13	W	24.2	7.2	1723	861.0	190.2	17.2	60.8	73.9		82.2	273.0	600.0	496
16	R21	S	22.3	6.6	1711	854.0	138.7	8.8	76.8	114.5		41.1	300.9	552.0	666
17	*MV UC	W	20.7	8.0	1060	521.0	95.3		40.0	24.3		1.4	191.2	408.0	304
18	*V02	S	8.5	7.2	2310	1501.5	>100.0	17.0	149.1	165.0	90.0	74.9	515.0	1166.0	1004
19	*V03	S	9.2	7.1	360	234.0	21.0	3.0	26.4	19.9	69.0	11.4	47.0	185.0	164
20	*V04	S	18.4	7.5	744	483.6	>100.0	9.0	33.1	22.1	55.0	52.1	51.5	304.0	236
21	*V05	S	21.0	7.8	640	416.0	42.0	10.0	46.9	37.8	83.0	9.7	30.0	323.0	242
22	*V06	S	18.3	7.8	1264	821.6	>100.0	7.0	56.7	107.0	75.0	61.9	119.0	678.0	510
23	*V07	S	19.3	7.5	1290	838.5	>100.0	7.0	52.4	111.0	78.0	63.3		615.0	479
24	*V08	S	10.5	7.3	366	237.9	22.0	4.0	31.6	21.6	74.0	42.8	48.0	169.0	138
25	*V09	S	20.9	8.3	1680	1092.0	>100.0	23.0	93.1	63.1	72.0	79.0	389.0	444.0	327
26	CA 10	S	21.0	6.9	2340	1576.0		7.0	91.8	168.2		50.0	878.0	320.0	300
27	CA 11	S	47.0	8.3	5145	3408.0		4.7	253.3	94.0		1633.0	96.0	140.0	103
28	*LC UC	W	20.7	7.9	1060	521.0	121.0		30.4	60.3		5.7	186.7	285.6	213
29	*LG UC	W	20.9	6.5	1586	789.0	135.5		65.6	99.1		2.8	297.4	265.2	335

Spring = S; Well = W

Only samples with dissolved SiO<sub>2</sub> were used for calculations in the WATCH and PHREEQC programs. CO<sub>2</sub> calculated according to Drever equation (1988) for all the samples.

\*TDS calculated according to Rusydi's equation (2018)

The highest values of EC and Cl were measured in CA11, sampled from the Kunugyaku hot spring in 2016, with 5145  $\mu\text{S}/\text{cm}$  and 1633 ppm, respectively. Similar values of EC and Cl were reported 6 years before from the same location (sample E28). The sampling temperature measured (47°C) is the same in both years. When high EC values were measured, the values of Na and Ca were also higher compared to the rest of the water samples. In EUI46, Na, and Ca have a maximum concentration of 682 ppm and 320 ppm, respectively. This water was sampled in 1992 from the Kunugyaku hot spring like the samples CA11 and E28.

The average SiO<sub>2</sub> content is 71 ppm, the maximum concentration of 90 ppm was found in sample V02 and the minimum of 48.2 ppm in sample EUI46. These samples are located on the southwest and northwest flanks of the Chimborazo volcano, respectively.

#### 4.1.1 Piper-Hill-Langelier diagram

In this diagram a total of 21 samples are included, shown in Figure 3. The samples that are distributed along the left field 1 have a composition that is dominated by the alkaline elements (Ca and Mg) rather than the alkali elements (Na and K).

In the central rhomboid field, the majority of the samples are in field 5, therefore the waters are mostly HCO<sub>3</sub>-Ca (weakly acid), associated with shallow water circuits (cold or warm meteoric waters), consisting of alluvial deposits, volcanic materials, and outcropping or subsurfacing carbonatic formations (IGME, 1985). Ellis and Mahon (1977) state that these waters could be derived from steam rich in CO<sub>2</sub> that condenses or mixes with water. This water is quite common in old geothermal waters or in the peripheries of geothermal areas in drains. They are usually in equilibrium and can be used to predict subsurface properties.

Only two samples, located in Kunugyaku (E28 and EUI46), were classified as Cl-Na. These qualities are associated with primary geothermal fluids and deeper circulation processes, as well as an interaction with the rocks of the regional basement (IGME, 1985), which is of alkaline-calc affinity with a high concentration in TDS (>1000 ppm) (Inguaggiato et al., 2010).

The rest of the samples are in field 9 and have mixed cationic and anionic characteristics.

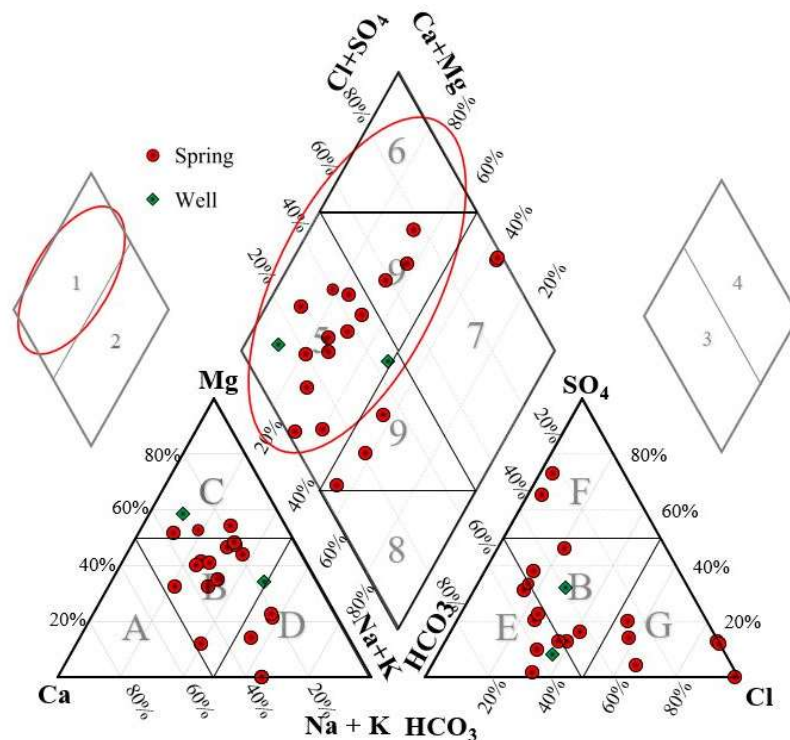


FIGURE 3: The Piper diagram for twenty-one water samples in study area. The red circles show the predominance of alkaline, HCO<sub>3</sub>-Ca type waters.

#### 4.1.2 Cl-SO<sub>4</sub>-HCO<sub>3</sub> diagram

This ternary diagram, shown in Figure 4, contains anionic information from 26 samples. A significant number of the samples is in the HCO<sub>3</sub> apex. Three groups are observed, one along the HCO<sub>3</sub>-Cl axis (R3, CN3, CN4, CN5, E29, E30, V04, V05, V06), defined as peripheral waters, another along the HCO<sub>3</sub>-SO<sub>4</sub> axis (LC UC, MV UC, LG UC, CA10, CN2, E31, IN64, R21, R7, V02, V03, V08, V09), classified as steam-heated waters, and the last group in the Cl apex (EUI46, E28, CA11), denoted as mature waters.

The peripheral waters comprise of eight springs and one well whose locations distinguish the edge of the geothermal reservoir. These waters are distributed around Guano, Chambo, Villa La Unión, and the community of Llío.

Ten springs and three well samples defined as steam-heated waters are located around Riobamba and Guano (CA10, CN2, E31, IN64, LC UC, LG UC, MV UC, R21, V09), around Llío (R07, V08) as well as on the southern flank of the Chimborazo volcano (V02, V03). These waters have no memory of the geothermal reservoir, therefore, geothermometry is not recommended (Giggenbach, 1991). Some steam-heated samples (CN2, R7, R21, CA10, LG UC) have slightly acidic (pH 5.8-6.9; section 3.1) characteristics that could be derived from steam rich in CO<sub>2</sub> that condensed or mixed with water (Ellis and Mahon, 1977).

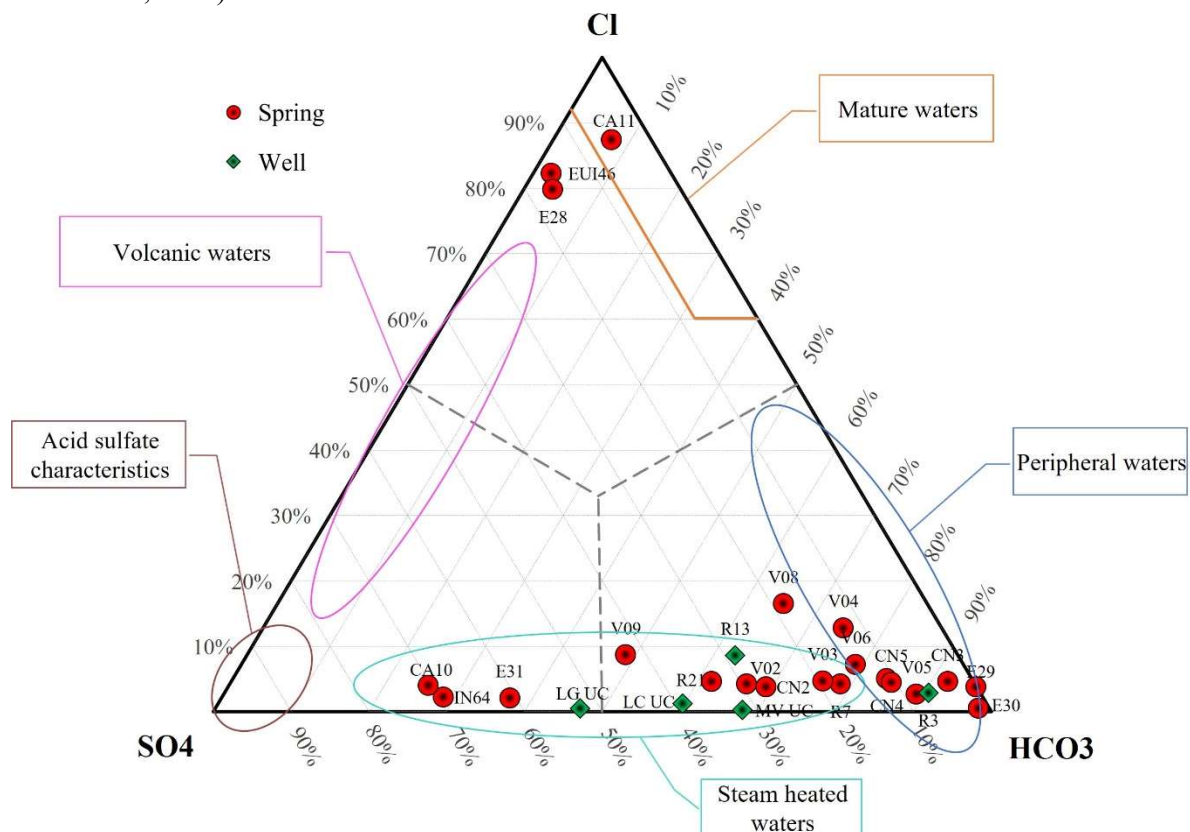


FIGURE 4: The Cl-SO<sub>4</sub>-HCO<sub>3</sub> ternary diagram for 26 thermal water samples in the study area

The mature waters (EUI46, E28, CA11) are on the northern flank of the Chimborazo volcano. This classification is consistent with the Cl-Na classification by the Piper diagram (Figure 3), indicating that these waters represent the fluid of the deep reservoir.

The groups of samples from the peripheries and mature waters can be used in geothermometry to estimate the temperature of the reservoir (Fournier, 1977; Giggenbach, 1991; Arnórsson, 1985). The results from geothermometry are presented in the following section.

## 4.2 Reservoir temperature estimation

### 4.2.1 Na-K-Mg geothermometer

In the ternary diagram of the Na-K-Mg geothermometer (Figure 5), 24 water samples were used. Most of them are in the Mg apex and are therefore classified as immature waters, which were previously classified as peripheral waters and steam-heated waters (Figure 4). This could be due to mixing with groundwater, acidic characteristics, or significant enrichment with CO<sub>2</sub> (Ellis and Mahon, 1977; IGME, 1985; Giggenbach, 1991).

Two spring samples, EUI46 and E28, are classified as waters in partial equilibrium and are located on the northern flank of the Chimborazo volcano. Possible reservoir temperatures of 100°C and 110°C can be extrapolated from EUI46 and E28, respectively. This agrees with the Piper diagram classification (Cl-Na type waters associated with primary geothermal fluids; Figure 3) and with the Cl-SO<sub>4</sub>-HCO<sub>3</sub> ternary diagram where these samples were classified as mature waters (Figure 4). This confirms that these waters are related to the deep reservoir.

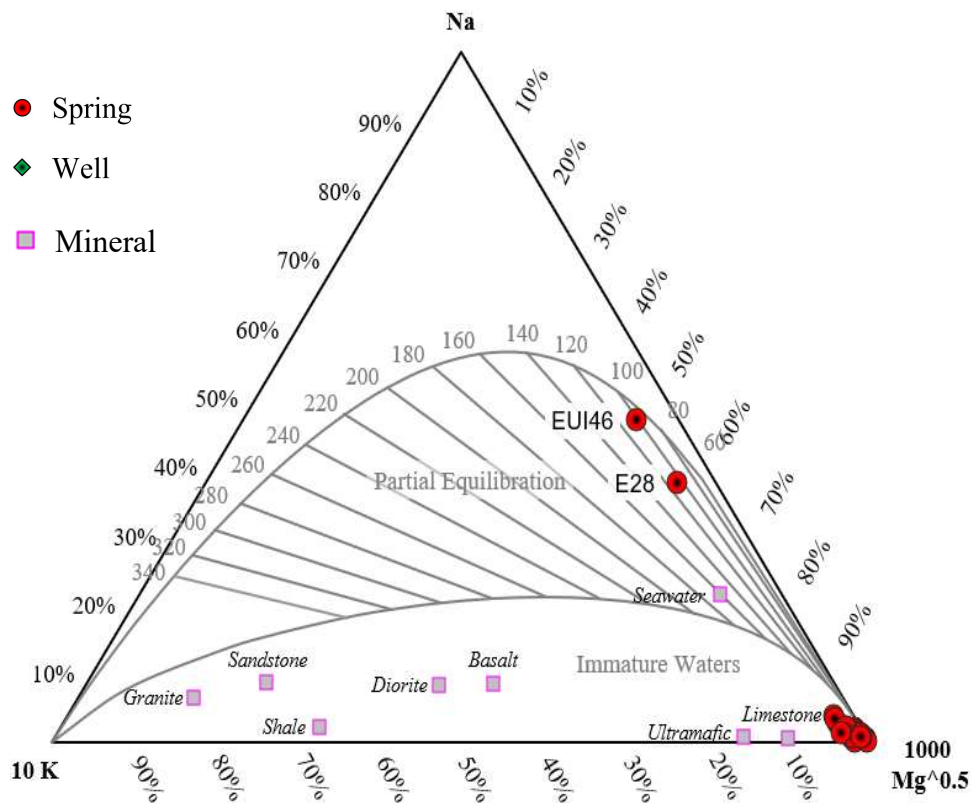


FIGURE 5: The Na-K-Mg ternary diagram for twenty-four thermal water samples in study area

### 4.2.2 Geothermometers of study area

Ten water samples, all from springs, were used to estimate temperatures based on cationic and SiO<sub>2</sub> geothermometers. The calculated reservoir temperatures are detailed in Table 3. Although the results of the Cl-SO<sub>4</sub>-HCO<sub>3</sub> diagram (Figure 4) gave indications on which samples were the most appropriate for geothermometry (mature and peripheral waters), all samples containing silica concentrations were included here. The results are described below.

Three of these samples (EUI46, V02, V03) are located on the flanks of the Chimborazo volcano while seven other samples were taken in vicinity of Villa La Unión, Guano, and Chambo. The temperatures

of the geothermometers vary widely and not all geothermometers are applicable to the study area. It is important to note that similarities between individual geothermometers help verify assumptions of equilibrium, thereby validating their results, while discrepancies indicate disequilibrium. However, these discrepancies can be used to quantify various processes in geothermal systems, such as boiling and mixing with cooler water in upstream zones. Hence, the different values obtained from each geothermometer will always be useful for the interpretation of results (Arnórsson, 2000).

Of the silica geothermometers, amorphous silica, alpha ( $\alpha$ ) and beta ( $\beta$ ) cristobalite, and quartz were discounted for the reasons described below, while the chalcedony geothermometer was determined the most appropriate silica geothermometer in this area.

Negative values were calculated from the amorphous silica geothermometer. According to Arnórsson (2000), this could be due to several factors. For example, this geothermometer tends to equilibrate in low temperature waters (<50°C) that have low pH or that have significant CO<sub>2</sub> concentrations. These characteristics do not apply to the samples of the study area since the pH is basic (7.1-8.3) and the calculated concentrations of CO<sub>2</sub> are on average 341 ppm (Table 3). Other reasons could be the sampling methodology, the precision of the chemical analyses, the laboratory methodologies used at that time, or the fact that the samples correspond to different years.

The  $\alpha$  and  $\beta$  cristobalite geothermometers were considered non-optimal for this study. According to Fournier and Rowe (1962), the former geothermometer works best in the temperature range of 100-150°C. As for the  $\beta$  cristobalite geothermometer, the calculated temperatures do not exceed 32°C, values that are lower than those measured on the surface (Table 4).

TABLE 4: Reservoir temperatures calculated from ten thermal water samples

Sample	Temperature of reservoir (°C)														
	Amorphous Silica	$\alpha$ Cristobalite	$\beta$ Cristobalite	Chalcedony conductive	Quartz conductive	Quartz adiabatic	Na-K-Ca	Na-K-Ca Mg corrected	Na-K Fournier et al., 1979	Na-K Truesdell, 1976	Na-K Giggenbach, 1988	Na-K Tonani, 1980	Na-K Nieva & Nieva, 1987	Na-K Arnorsson, 1983	K-Mg Giggenbach, 1986
EUI46	-15	50	3	<b>70</b>	101	101	52	52	80	31	<b>102</b>	49	70	43	97
IN64*	0	68	20	90	118	117	78	16	193	158	210	190	181	167	44
V02*	12	81	32	104	132	128	72	23	267	253	279	297	253	256	49
V03*	-1	67	19	89	118	116	41	41	250	229	262	270	236	234	35
V04	-10	56	9	<b>77</b>	107	106	84	33	208	176	224	210	195	184	56
V05	8	76	28	<b>99</b>	127	124	71	32	305	305	313	356	290	304	53
V06	3	71	23	93	122	120	65	18	188	152	205	183	176	161	35
V07	5	73	25	96	124	121	66	16	188	152	205	183	176	161	35
V08*	3	70	23	93	121	119	46	46	274	262	285	308	260	265	40
V09*	1	69	21	91	120	118	93	29	301	299	309	349	286	299	65

\* Classified as steam-heated waters

Values in bold correspond to the estimated temperature range of the reservoir and its edge

The red rectangle indicates the geothermometer chosen to estimate the reservoir temperature

The temperatures obtained with the two quartz geothermometers (conductive and adiabatic) are very similar to each other ranging from 101°C to 127°C. However, equilibrium with quartz has been found to control silica concentration in systems above 180°C and are not applicable. Chalcedony is the control phase at temperatures lower than 110°C, as observed in Icelandic geothermal fluids (Arnórsson et al., 1975). The estimated temperatures with chalcedony geothermometer range from 70 to 99°C.

Based on the results obtained from the Na-K-Mg geothermometer diagram (Figure 5) and some previous studies that estimated the geothermal potential of the area to be low enthalpy (IAEA, 1992; Beate, 2010; Ibarra et al., 2015; Jimbo, 2016), the cationic (Na-K-Mg) geothermometers were not considered for this study, with the exception of sample EUI46. The temperature range calculated for this sample was between a minimum of 43°C and a maximum of 102°C. However, the minimum value was discarded because the calculated temperature is less than the measured temperature at the surface (47.5°C; Table 3). The maximum value (102°C) is in close agreement with the extrapolated temperature from the Na-K-Mg geothermometer diagram (100°C; Figure 5).

Considering the fluid classifications and the equilibrium assumptions of the reservoir, two temperature ranges can be identified. The first of these ranges is for mature waters, represented by the EUI46 sample. The minimum temperature is 70°C (conductive chalcedony geothermometer) and the maximum temperature is 102°C (Na-K geothermometer from Giggenbach, 1988). The second temperature range valid for peripheral waters is 77 to 99°C, calculated using the conductive chalcedony geothermometer.

#### 4.3 Mineral saturation states

Issues in production wells can arise from the precipitation of minerals like calcite and amorphous silica. Silica deposition is a problem when geothermal waters are cooled enough through boiling, resulting in the supersaturation of amorphous silica (Ármansson et al., 2007). Using the chalcedony geothermometer as the reference temperature (Table 3), the mineral saturation states were calculated for calcite and amorphous silica, shown in Figure 6, to examine potential scaling issues upon utilization. Note that samples IN64, V02, V03, V08, and V09 are classified as steam-heated waters (Figure 4), therefore this method is not ideal for determining potential scaling issues since they are not representative of the geothermal fluid.

The saturation state with respect to amorphous silica increases for all samples upon cooling. When the samples cool down to 19°C or below (Table 4), the precipitation of amorphous silica is possible except for EUI46. This is a typical issue for high enthalpy fields and the main obstacle to efficient extraction of fluids. Silica deposits cause operational problems when forming in surface equipment and reinjection wells (Gunnarsson and Arnórsson, 2005). The results show that in this case, silica scaling is not likely during fluid extraction and only if the fluids are significantly cooled.

As the fluids cool, the saturation state with respect to calcite decreases for all samples. Calcite scaling would occur in fluids from V03, V04, and V08 at 85, 65 and 25°C, respectively (Table 5). There could be potential scaling in EUI46 if fluids are completely cooled to less than 20°C. The rest of the fluids are supersaturated with respect to calcite throughout cooling. Precipitation of calcite typically occurs in the reservoir, particularly around the wells (Crabtree and Johnson, 2009), although most studies focus on its deposition in production wells (Satman et al., 1999). Calcite scaling can also be deposited along the pipelines from the injection wells to the surface equipment, blocking normal flow of the water as well as the production equipment (Crabtree and Johnson, 2009). Furthermore, when calcite precipitates it causes a greater pressure drop, which in turn leads to more precipitation (Satman et al., 1999).



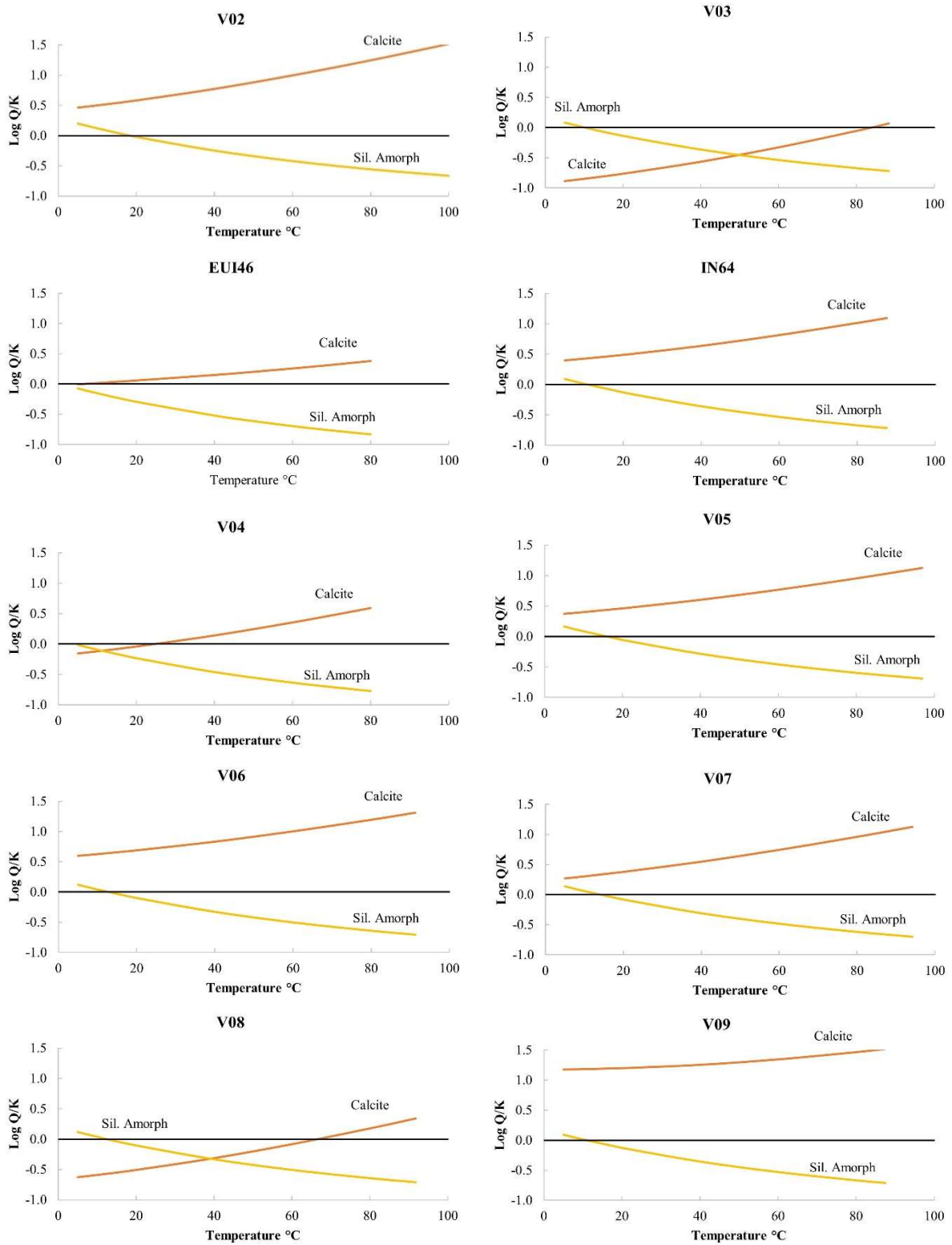






FIGURE 6: Saturation states ( $\log Q/K$ ) of the geothermal waters from 10 sites with respect to amorphous silica and calcite as a function of temperature

TABLE 5: Equilibrium temperature for the SI of amorphous silica and calcite for 10 water samples

Sample	Amorphous silica Equilibrium T (°C)	Calcite Equilibrium T (°C)
	Oversaturation  Undersaturation 	Oversaturation  Undersaturation 
EUI46		5
IN64*	10	
V02*	19	
V03*	10	85
V04	5	25
V05	16	
V06	13	
V07	15	
V08*	13	67
V09*	10	

\* Classified as steam-heated waters

## 5. IMPLICATIONS FOR GEOTHERMAL UTILIZATION

Although there were some inconsistencies in the present study, two well-defined areas can be identified. The area around Kunugyaku has alkaline, Cl-Na, mature waters, an estimated reservoir temperatures between 70-102°C, and a surface temperature of 47°C. Another area located around Riobamba and southeast of Guayllabamba has peripheral waters (“immature”) with surface temperatures of 18-38°C and estimated reservoir temperatures of 77-99°C. Steam-heated waters are dispersed throughout the study area with surface temperatures of 19-38°C, although mostly located near Guano.

These results are in partial agreement with previous studies (Beate, 2010; Carrasco and Naula, 2012; Ibarra et al., 2015; Jimbo, 2016). Ibarra et al. (2015) and Jimbo (2016) also estimated reservoir temperatures at 83-107°C, which are like those calculated in this study. This work does verify that the area has a low enthalpy geothermal reservoir, but more research is needed to better understand the dynamics of the geothermal system.

Given the possibility that this geothermal resource will be used in the future, the following aspects must be considered. The saturation states with respect to amorphous silica show possible supersaturation and therefore potential scaling problems upon cooling below 5-16°C around Riobamba city. Amorphous silica deposits could be forming on the surface of equipment and reinjection wells, clogging pipes, and reducing production capacity (Gunnarsson and Arnórsson, 2005).

Calcite scaling could also occur in the reservoir and during exploitation of almost all springs. At the Kunugyaku hot spring (EUI46), on the southern flank of the Chimborazo volcano (V03), northwest of Chambo (V04), and northwest of San Andrés (V08) scaling could occur at temperatures of around 5, 85, 25, and 67°C, respectively. In these cases, economic chemical techniques could be utilized to remove scaling. Conventional mechanical methods which are considered more efficient in removing scaling from pipes, although more expensive, could also be applied (Crabtree and Johnson, 2009).

Due to the alkaline characteristics of the fluids, potential issues caused by corrosion were not considered.

According to Línal (1973) and the evaluation of the geochemical results in the study area, there are

multiple possible applications for direct use of the geothermal energy, which thus far have been mostly limited to balneology (Beate et al., 2020). The first greenhouse utilizing geothermal water in the Chimborazo province was built in 2018 in Calpi (a town 10 km to the west of Riobamba) with promising results (IIGE, 2020). Jimbo (2016) also suggested that the waters of Kunugyaku and Guayllabamba, in the northwest and southeast of the study area, respectively, could be used for space heating, food dehydration and fish farming.

Based on the reservoir temperatures estimated in this study, the geothermal fluids can be directly utilized for geothermal heat pumps for greenhouses, fruit and vegetable drying, carbonation of soft drinks, food processing, building heating and cooling, blanching, cooking, and pasteurization. Cooler fluids could also be utilized for mushroom cultivation, aquaculture, biogas production, and soil warming. Further study would be needed to determine if direct uses, such as binary geothermal power generation, could be applied.

With agriculture being a big industry in the study area and the first greenhouse project in the province a success, it is especially recommended to operate greenhouses using geothermal heat pumps. This application is very efficient and can produce very high yields in products such as vegetables, flowers, and others. Heated greenhouses also allow for the intensive use of the soil and help to control plant health. Moreover, from an economic point of view, profits would increase as the typical growing season of crops can be expanded (Adaro et al., 1999).

Although Chimborazo is on the national priority list of geothermal exploitation, the geochemical information that is available dates back more than thirty years and chemical composition analysis is incomplete. Therefore, to enable future development and utilization of the geothermal resources, it is essential to conduct new exploration studies. The explored area should include the surroundings of Riobamba and the San Francisco-Guayllabamba hot springs, located in the southeast of the study area. Furthermore, it is recommended that a full geochemical analysis including trace metals is conducted in future geochemical surveys to determine whether pre-treatment of the fluids is required, particularly for direct utilization.

## 6. CONCLUSIONS

- The results of this study are partially consistent with the previous research. It verifies that this area has a low enthalpy geothermal reservoir. In addition, the reservoir temperatures calculated in previous years are similar to those estimated here.
- Kunugyaku hot spring has alkaline, Cl-Na, mature waters with estimated reservoir temperatures of 70-102°C based on the chalcedony and cationic geothermometers.
- Waters from the periphery of the geothermal reservoir are located near the city of Riobamba and southeast of the town of Guayllabamba with estimated reservoir temperatures of 77-99°C based on the chalcedony geothermometer.
- Steam-heated waters, although mostly near the city of Guano, are dispersed throughout the study area and have surface temperatures of 19-38°C. These waters are not directly related to the fluid of the deep reservoir, and its use is only recommended if further studies verify this classification.
- Evaluation of the fluid compositions suggest possible calcite scaling at temperatures of 25-85°C and potential scaling of amorphous silica if the fluids are significantly cooled below 20°C.
- The lack of analytical parameters such as anions, major cations, and silica limits the application of geochemical methods (ternary diagrams, geothermometry, and mineral saturation states) and therefore possibly decreased the precision of this study's geochemical evaluation.
- The results suggest that the geothermal fluids in the northwestern Chimborazo province can be utilized beyond balneology, such as for greenhouse air conditioning, to develop the agricultural sector.

## ACKNOWLEDGEMENTS

First, my respect and gratitude goes to Marcelo Moya, Director of Technology Transfer and Incubation of the Institute of Geological and Energy Research of Ecuador, who trusted me and made it possible for me to take part in this prestigious program. Sincere thanks to the Government of Iceland for promoting and facilitating these training spaces. Thanks to the staff of the GRÓ GTP: Ingimar Haraldsson, my angel Vigdís Harðardóttir, Guðni Axelsson, the sweet Málfríður Ómarsdóttir, and Markús Wilde. Each of them has made this experience memorable and worthwhile. Sincere thanks to my teachers for their patience, vocation, and love of their work, to Finnbogi Óskarsson, and my supervisors Deirdre Clark and Iwona Galeczka.

## NOMENCLATURE

#	Number
%	Percent
AECID	Spanish Agency for International Development Cooperation
a.k.a.	also known as
ARCERNNR	Agency for the Regulation and Control of Energy and Non-Renewable Natural Resources
Ca	Calcium
CaCO <sub>3</sub>	Calcite
Cl	Chloride
cm	Centimetres
CO <sub>2</sub>	Carbon Dioxide
CO <sub>3</sub>	Carbonate
e.g	For example
EC	Electrical Conductivity
ESPOCH	Polytechnic School of Chimborazo
EPN	National Polytechnic School
Fe	Iron
GAD	Decentralized Autonomous Government
GDP	Gross Domestic Product
GWh	Gigawatt hour
HCO <sub>3</sub>	Bicarbonate
i.e.	That is
IIGE	Geology and Energy Research Institute
INECEL	Ecuadorian Institute of Electrification
INER	National Institute of Energy Efficiency and Renewable Energies
IPA	Agricultural Productivity Index
JICA	Japan International Cooperation Agency
K	Potassium
Km	Square kilometre
L/s	Litres per second
m	Metre
m.a.s.l	Meters above sea level
MEER	Ministry of Electricity and Renewable Energy
Mg	Magnesium
mg/L	Milligrams per litre
MWe	Megawatt electric
MWt	Megawatt thermal
Na	Sodium
°C	Degrees Celsius
OH	Hydroxyl Radical

IAEA	International Atomic Energy Agency
OLADE	Latin American Energy Organization
ppm	Parts per million
SiO <sub>2</sub>	Silica
SO <sub>4</sub>	Sulphate
T	Temperature
TDS	Total Dissolved Solids
TJ	Tera Joule
yr	year
μS/cm	MicroSiems per centimetre

## REFERENCES

- Adaro, J.A., Galimberti, P.D., Lema, A.I., Fasulo, A., Barral, J.R., 1999: Geothermal contribution to greenhouse heating. *Applied Energy*, 64, 241-249.
- ARCERNNR, 2021: *National electric energy balance as of August 2021*. Agency for the Regulation and Control of Energy and Non-Renewable Natural Resources, Quito, 1 pp.
- Ármannsson, H., Fridriksson, Th., Wiese, F., Hernández, P., and Pérez N., 2007: CO<sub>2</sub> budget of the Krafla geothermal system, NE-Iceland. *Proceedings of the 12<sup>th</sup> International Symposium on Water-Rock Interaction 2007*, Taylor & Francis Group, London, 189-192.
- Arnórsson, S., 1985: The use of mixing models and chemical geothermometers for estimating underground temperature in geothermal systems. *J. Volc. Geotherm. Res.*, 23, 299-335.
- Arnórsson, S., 2000: Mixing processes in upflow zones and mixing models. In: Arnórsson, S. (ed.), *Isotopic and chemical techniques in geothermal exploration, development and use. Sampling methods, data handling, interpretation*. International Atomic Energy Agency, Vienna, 200-211.
- Arnórsson, S., Gunnlaugsson, E., and Svavarsson, H., 1983: The chemistry of geothermal waters in Iceland II. Mineral equilibria and independent variables controlling water compositions. *Geochim. Cosmochim. Acta*, 47, 547-566.
- Arnórsson, S., Sigurdsson, S. and Svavarsson, H., 1982: The chemistry of geothermal waters in Iceland I. Calculation of aqueous speciation from 0°C to 370°C. *Geochim. Cosmochim. Acta*, 46, 1513-1532.
- Arnórsson, S., Stefánsson, V., Sigurmundsson, S., Gíslason, G., and Grönvold, K., 1975: *Exploration of the Svartsengi geothermal field*. Orkustofnun, Reykjavík, report OS-JHD-7541 (in Icelandic), 55 pp.
- Asimbaya, D.X., 2018: Geothermal energy update in Ecuador. *International Symposium on Earth Science and Technology 2018, Fukuoka, Japan*, 1-4.
- Baldock, J.W., 1982: *Geology of Ecuador*. Ministry of Natural Resources and Energy. General Directorate of Geology and Mines, Quito, Ecuador, 70 pp.
- Barbier, E., 2002: Geothermal energy technology and status: An overview. *Renewable and Sustainable Energy Reviews*, 6, 3-65.
- Beate, B., 2010: *Plan for the use of geothermal resources in Ecuador*. International Atomic Energy Agency, Ministry of Electricity and Renewable Energy, Quito, 175 pp.

- Beate, B., Uquizo, M. and Lloret, A., 2020: Geothermal country update of Ecuador: 2015-2020. *Proceedings of the World Geothermal Congress 2020, Reykjavik, Iceland*, 12 pp.
- Benítez, S., 1995: Geodynamic evolution of the South Ecuadorian coastal province in the Upper Cretaceous-Tertiary. *Geology Alpine*, 71, 3-163.
- Bjarnason, J.Ö., 2010: *The chemical speciation program WATCH, version 2.4*. ÍSOR – Iceland GeoSurvey, Reykjavik, website: [www.geothermal.is/software](http://www.geothermal.is/software).
- Carrasco, W. J. and Naula, W., 2012: *Characterization and preparation of an inventory of low enthalpy geothermal sources in the Province of Chimborazo and proposal for the creation of a geothermal energy research center at ESPOCH*. Chimborazo Polytechnic Superior School, Chimborazo, Bachelor thesis, 237 pp.
- Carrera, D. et al., 2016: Hydrogeochemical analysis of volcanic and geothermal fluids in the Andes from Ecuador using hydrochemical plots (Stiff, Piper and Schoeller-Berkaloff diagrams). *IOP Conference Series: Earth and Environmental Science*, 39, 1-9.
- Cioni, R. and Marini, L., 2020: *A thermodynamic approach to water geothermometry*. Springer Nature Switzerland AG, Switzerland, 426 pp.
- Crabtree, M. and Johnson, A., 2009: The fight against fouling - Removal and prevention. *Oilfield Review*, 11, 20 pp.
- D'Amore, F., Scandiffio, G. and Panichi, C., 1983: Some observations on the chemical classification of ground waters. *Geothermics*, 12, 141-148.
- Drever, J.I., 1988: *The geochemistry of natural waters*. Prentice Hall Englewood Cliffs, New Jersey, 437 pp.
- Ellis, A. J. and Mahon, A. J., 1977: *Chemistry and Geothermal Systems*. New York: Academic Press, 1977.
- EPN, 2021: *Active volcanoes in Ecuador*. Website: [www.igepn.edu.ec](http://www.igepn.edu.ec)
- Fournier, R.O., 1977: Chemical geothermometers and mixing model for geothermal systems. *Geothermics*, 5, 41-50.
- Fournier, R. O., Walther, J. V. and Helgeson, H. C., 1979: Calculation of the thermodynamic properties of aqueous silica and the solubility of quartz and its polymorphs at high pressures and temperatures, *American Journal of Science*, 279, 9, 1070–1082.
- Fournier, R.O., 1981: Application of water chemistry to geothermal exploration and reservoir engineering. In: Rybach, L., and Muffler, L.J.P. (editors), *Geothermal system: Principles and case histories*. John Wiley and Sons Ltd., Chichester, 109-143.
- Fournier, R.O., and Rowe, J.J., 1962: The solubility of cristobalite along the three-phase curve, gas plus liquid plus cristobalite. *Am. Mineralogist* 47, 897-902.
- GAD Chimborazo, 2015: *Development and territorial planning plan of the Province of Chimborazo*, Decentralized Autonomous Government of the Province of Chimborazo, Riobamba, report, 554 pp.
- GAD Tungurahua, 2017: *Technical report for the alignment of the Provincial PDOT territorial development and planning plan to the national development plan 2017-2021*, Decentralized

Autonomous Government of the Province of Chimborazo, Ambato, report, 160 pp.

Gehring, M. and Loksha, V., 2012: *Geothermal handbook planning and financing power generation, World Bank technical report*. Energy Sector Management Assistance Program (ESMAP), Washington DC, 002/12, report, 94 pp.

Giggenbach, W.F., 1986: Graphical techniques for the evaluated water/rock equilibration conditions by use of Na, K, Mg and Ca contents of discharge water. *Proceedings of the 8<sup>th</sup> New Zealand Geothermal Workshop, Auckland, NZ*, 37-43.

Giggenbach, W.F., 1988: Geothermal solute equilibria. Derivation of Na-K-Mg-Ca geothermometers. *Geochim. Cosmochim. Acta*, 52, 2749-2765.

Giggenbach, W.F., 1991: Chemical techniques in geothermal exploration. In: D'Amore, F. (coordinator), *Application of geochemistry in geothermal reservoir development*. UNITAR/UNDP publication, Rome, 119-144.

Gunnarsson, I. and Arnórsson S., 2005: Impact of silica scaling on the efficiency of heat extraction from high-temperature geothermal fluids. *Geothermics*, 34, 320-329.

IAEA, 1992: *Geothermal investigations with isotope and geochemical techniques in Latin America*. International Atomic Energy Agency, San José de Costa Rica, IAEA-TECDOC-641, 452 pp.

Ibarra D., Mendoza B., Asimbaya D., Vaca R., and Jimbo G., 2015: Geochemical and hydrogeological characterization for geothermal exploitation in the Province of Chimborazo. *International Congress R+D+i in Energy Sustainability INER, Quito, Ecuador*, 10 pp.

IIGE, 2020: Energy sustainability in greenhouses. *Scientific popularization magazine La Linterna. Special Edition International Congress R+D+i Energy Sustainability*, no. 004, 22-25.

IGME, 1985: *Methodological analysis of the geochemical techniques used in geothermal prospecting*. Geological and Mining Institute of Spain. 417 pp.

INAMHI, 2013: *Thermomineral waters in Ecuador*. National Institute of Meteorology and Hydrology INAMHI, Quito, 96 pp.

INEC, 2021: *National Institute of Statistics and Censuses, Population and Demographics*, website: <https://www.ecuadorencifras.gob.ec/censo-de-poblacion-y-vivienda/>

Inguaggiato, S., Hidalgo, S., Beate, B., and Bourquim, J., 2010: Geochemical and isotopic characterization of volcanic and geothermal fluids discharged from the Ecuadorian volcanic arc. *Geofluids*, 10, 525-541.

Jimbo, G.A., 2016: *Preliminary geological-geochemical evaluation of the geothermal prospect 'Chimborazo', with application of remote sensors*. University of Guayaquil, Guayaquil, Bachelor thesis, 125 pp.

Lazo, C., 2015: *Tourist geography of Ecuador*. Technical University of Machala, Machala, 72 pp.

Lindal, B., 1973: Industrial and other applications of geothermal energy, except power production and district heating. *Geothermal Energy, Paris, UNESCO, LC 7297*, 135-148.

MEER, 2010: *Plan for the use of geothermal resources in Ecuador*. Ministry of Electricity and Renewable Energy, Quito, 177 pp.

- Muffler, P. and Cataldi, R., 1978: Methods for regional assessment of geothermal resources. *Geothermics*, 7, 53–89.
- Nieva, D., and Nieva, R., 1987: Developments in geothermal energy in Mexico, part 12-A: Cationic composition geothermometer for prospection of geothermal resources. *Heat Recovery Systems and CHP*, 7, 243-258.
- National Assembly of Ecuador, 2008: *Constitution of the Republic of Ecuador, National Assembly of Ecuador, Quito*, website: <https://www.asambleanacional.gob.ec/es/contenido/constitucion-de-la-republica-del-ecuador-2008-reformada>, 216 pp.
- Parkhurst, D.L., Thorstenson, D.C., and Plummer, L.N., 1980: *PHREEQE – A computer program for geochemical calculations*. U.S. Geological Survey Water-Resources Investigations Report 80-96 (revised and reprinted August, 1990), 195 pp.
- Piper, A.M., 1944: A graphic procedure in the geochemical interpretation of water-analyses. *Am. Geophys. Union, Trans.*, 25, 914-923.
- Powell, T., and Cumming, W., 2010: Spreadsheets for geothermal water and gas geochemistry. *Proceedings of the 35<sup>th</sup> Workshop on Geothermal Reservoir Engineering, Stanford University, Stanford, CA*, 10 pp.
- Reino, S. J., 2013: *Study of the underground waters of the city of Riobamba and its areas of influence: Baseline*. Chimborazo Polytechnic Superior School, Chimborazo, Bachelor thesis, 145 pp.
- Romano, P. and Liotta, M., 2020: Using and abusing Giggenbach ternary Na-K-Mg diagram. *Chemical Geology*, 541, 6 pp.
- Rusydi, A.F. 2018: Correlation between conductivity and total dissolved solid in various type of water: A review. *IOP Conference Series: Earth and Environmental Science*, 118, 6 pp.
- Satman, A., Ugur, Z. and Onur, M., 1999: The effect of calcite deposition on geothermal well inflow performance. *Geothermics*, 28, 425-444.
- Tonani, F., 1980: Some remarks on the application of geochemical techniques in geothermal exploration. *Proceedings, Adv. Eur. Geoth. Res., 2<sup>nd</sup> Symposium, Strasbourg*, 428-443.
- Truesdell, A.H., 1976: Summary of section III - geochemical techniques in exploration. *Proceedings of the 2<sup>nd</sup> U.N. Symposium on the Development and Use of Geothermal Resources, San Francisco, 1*, liii-lxxix.
- Tschopp H., 1953: Oil explorations in the Oriente of Ecuador, 1938-1950. *Bulletin of the American Association of Petroleum Geologists*, 10, 2303-2347.
- Urresta, E., Moya, M., Campana, C. and Cruz, C., 2021: Ground thermal conductivity estimation using the thermal response test with a horizontal ground heat exchanger, *Geothermics*, 96, 8 pp.
- Vallejo, C. et al., 2009: Mode and timing of terrane accretion in the forearc of the Andes of Ecuador. *The Geological Society of America, Memoir 204*, 197–216.
- Voigt, M., Marieni, C., Clark, D.E., Gislason, S.R., Oelkers, E.H., 2018: Evaluation and refinement of thermodynamic databases for mineral carbonation. *Energy Procedia*, 146, 81–91.



**APPENDIX I: Geographical location of the water samples in the study area**

N°	Code	Reference	Sample name	X	Y
1	72M18	Jimbo, 2016	72M18 INERHI 1984		
2	72M19	Jimbo, 2016	72M19 INERHI 1984		
3	EUI46	OIEA, 1992	Kunugyaku	737337	9852468
4	E28	Inguaggiato et al., 2010	Kunugyaku	737470	9851990
5	E29	Inguaggiato et al., 2010	Timbul river	772993	9801831
6	E30	Inguaggiato et al., 2010	Timbul river	765913	9820911
7	E31	Inguaggiato et al., 2010	Los Elenes	765913	9820911
8	CN2	Carrasco et al., 2012	Los Elenes thermal water	766063	9822367
9	CN3	Carrasco et al., 2012	Guayllabamba thermal water	769146	9808141
10	CN4	Carrasco et al., 2012	Pantus thermal water	765006	9809916
11	CN5	Carrasco et al., 2012	Conugpogyo thermal water	747940	9811065
12	IN64	INAMHI, 2013	Los Elenes	765919	9820912
13	R3	Reino, 2013	Llio #5 well	754449	9827230
14	R7	Reino, 2013	San Pablo #2	753952	9827172
15	R13	Reino, 2013	Yaruquíes-El Estadio well	758994	9813514
16	R21	Reino, 2013	Los Elenes	758994	9813514
17	MV UC	Jimbo, 2016	San Martin de Veranillo	764359	9816828
18	V02	Jimbo, 2016	INER	739797	9831563
19	V03	Jimbo, 2016	INER	740749	9832213
20	V04	Jimbo, 2016	INER	764516	9810141
21	V05	Jimbo, 2016	INER	748095	9810985
22	V06	Jimbo, 2016	INER	766395	9820367
23	V07	Jimbo, 2016	INER	766650	9820076
24	V08	Jimbo, 2016	INER	753938	9827175
25	V09	Jimbo, 2016	INER	759003	9813510
26	CA 10	Carrera, 2016	Los Elenes	765936	9820936
27	CA 11	Carrera, 2016	Kunugyaku	737473	9851990
28	LC UC	Jimbo, 2016	Los Chingazos	769032	9822158
29	LG UC	Jimbo, 2016	Langos well	760132	9822180

WGS84 Reference System, UTM 17S Projection